Proceedings of the Canadian Society for Mechanical Engineering International Congress 2020
CSME Congress 2020
June 21-24, 2020, Charlottetown, PE, Canada

Numerical simulation of the capture efficiency of a domestic range hood for different burner scenarios

Alla Eddine Benchikh Le Hocine, Sébastien Poncet, Hachimi Fellouah
Department of Mechanical Engineering
Université de Sherbrooke
2500 Boul. de l'Université, Sherbrooke (QC) J1K 2R1 Canada
Email: alla.benchikh.le.hocine@USherbrooke.ca

***Abstract*—Exposure to cooking fumes has been found to cause adverse health effects. In some conditions, cooking is more dangerous than other sources of air pollution. Multiple studies have been conducted to improve the pollutant extraction by the kitchen range hoods. In the present study, numerical simulations were performed to model the extraction of the CO_2 by a kitchen hood for different burners configurations. A new developed OpenFoam solver was used. The new solver is based in a buoyant boussinesq and the turbulent passive scalar transport solvers. For configuration 1, a linear relation was observed between the capture efficiency and the fan flow rate between 100 cfm and 337 cfm. Above 337 cfm, all the pollutants are captured by the hood. A decrease in the capture efficiency is observed by turning on more burners. For configuration 2, a non-uniform scattered CO_2 distribution is observed between the stove and the hood. A jet like flow pattern toward the fan inlet was found in configurations 3 and 4. A discrepancy in the temperature distribution near to the fan inlet is distinguishable between the different configurations.**

***Index Terms*—OpenFoam, turbulent passive scalar, RANS, MRF, Heat transfer**

I. Introduction

In nowadays, the kitchen hood industry is marked by a strong competition between the different constructors. Their main objectives are to deliver a highly efficient hood in terms of pollutant capture with the lowest generated sound by the rotating fan. In addition, different directives have been established for building in terms of thermal comfort and pollutant dispersion. Furthermore, multiple studies found a significant correlation between the particles emitted from cooking activity in kitchen and lung cancer, chronic obstructive pulmonary disease (CODP) and diabetes [1]–[4]. Those stated conditions and restrictions drive the researches to study numerically and experimentally the efficiency of the kitchen hoods.

To perform the kitchen hood capture efficiency many studies have been conducted numerically and experimentally. Cao et $al.$ [5] found that the integration of a makeup air system in a kitchen can reduce the exposure level of the occupants. They also found that the required flow rate for upward makeup air is less than the downward system. Yi et $al.$ [6] studied experimentally and numerically the effect of the air volume variation on the performance of the concurrent supply and exhaust ventilation. Yi et $al.$ [6] observed an increase of the capture efficiency with the exhaust air rate of the range hood. Tseng and Chen [7] studied experimentally with flow visualizations and nanoparticle measurements the influence of the turbulent structures to the particulates generated from cooking oils for a wall-mounted range hood and an island hood. They found that the regions where the large-scale turbulent vortices are dominant were more prone to dispersion of ultrafine particles due to the complex interaction between the shear layers and the suction stream. Lee et $al.$ [8] introduced a new hood with a vortex ventilator (VV), the idea is to force the generation of a vortical flow to improve the capture efficiency of the pollutant. The result showed that the VV improved by 70% the capture efficiency compared to a basic hood system. Huang et $al.$ [9] investigated experimentally the spillage levels relative magnitude for wall-mounted and jet-isolated range hoods. Huang et $al.$ [9] found that increasing the jet-isolated flow rate can reduce moderately the spillage levels. In industrial production, the push-pull ventilation is widely used [10], [11], but it is rarely used for pollution control in the kitchen. Zhou et $al.$ [12] proposed a push-pull ventilation system for a residential kitchen, and they observed a capture efficiency improvement with a good air distribution in the kitchen area.

Most of the conducted studies in the state of the art in kitchen range hoods capture efficiency have been performed with only one burner on. However, in real life, the cooking activity requires the use of different burners in same time, especially in family houses. The idea of the present work is to perform numerical simulation in order to predict the capture efficiency of a kitchen hood with a rotating fan in different configurations of burners ignitions.

Numerical modelling

In order to model the CO_2 released from the burners, a new 3D steady-state Navier-Stokes incompressible flow solver including the transport of a turbulent passive scalar was developed. The open source openFoam (4.1) was used to implement the new solver.

In order to check the efficiency of the hood capture in different conditions, four configurations of burners ignition are tested (Fig. 1): 1) configuration1: burner 1 on ; 2) configuration 2: burners 1 and 2 on ; 3) configuration 3 : burners 1,2 and 3 on; 3) configuration 4: all burners on.

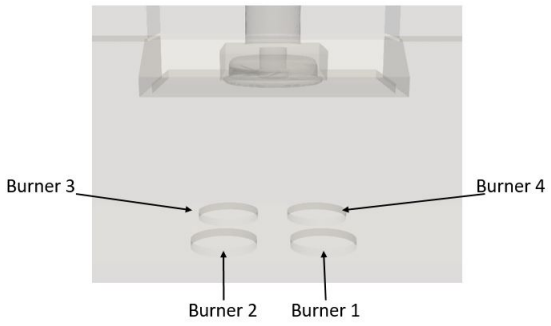

Fig. 1. 3D sketch of the different burners.

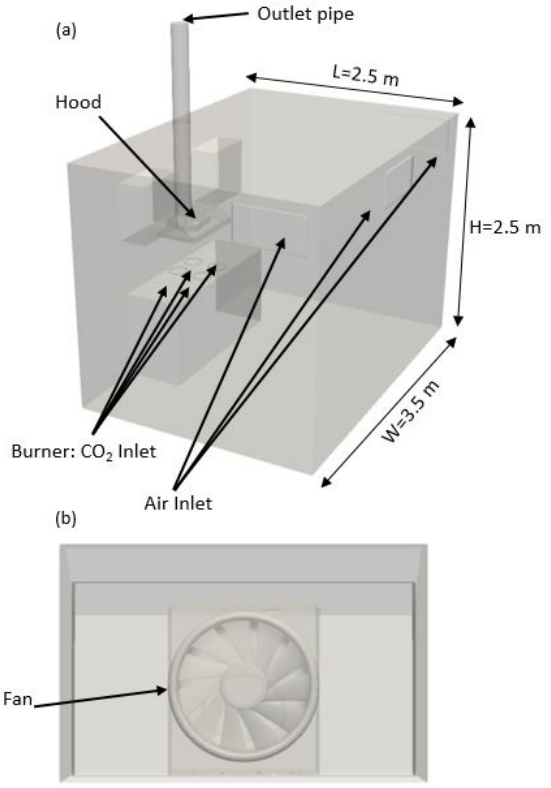

Fig. 2. (a) Sketch of the computational domain and (b) the rotating fan.

GEOMETRICAL MODELLING

Figure 2 presents a sketch of the computational domain. The whole kitchen is constructed by respecting the E3087−18 [13] norm. The length, width and height of the kitchen are $L = 2.5$, $W = 3.5$ and $H = 2.5$ m, respectively. The CO_2 is captured by an eleven bladed axial fan (diameter of 0.28 m) as shown in Fig. 2. Three rectangular entries with the following dimensions: length 0.7 m and width 0.35 m introduce the fresh air to the kitchen.

New OpenFoam Solver

The transport of the turbulent passive scalar CO_2 was implemented in the BuyontBoussinesqSimpleFoam solver, because the following aspects exist already in this solver: (i) the multiple reference frame (MRF) approach to model the rotating fan; (ii) the energy equation to model the heat transfer between the released CO_2 and the ambient air; (iii) the solver is steady and so the calculation time is reduced.

The passive scalar approach is based on the hypothesis that the densities of air and CO_2 are quite comparable ($\rho = 1.12$ and 1.37 kg/m^3 for air and CO_2 respectively). The turbulent transport of the passive scalar, here CO_2, is represented by the convective-diffusive equation as follows:

$$\nabla.(\mathbf{U}C) - \nabla^2(D_{eff}C) = 0 \tag{1}$$

The CO_2 voluminal fraction in the calculated volume is represented by the C parameter in Eqn. (1) which varies between 0 and 1. The transport of the turbulent passive scalar is conducted by two main terms: the convective term ($\nabla.(\mathbf{U}C)$) represents the transport of the passive scalar by the velocity field $\mathbf{U}$. The second term ($\nabla^2(D_{eff}C)$) is the diffusion of the passive scalar in the surrounding domain by introducing a binary diffusion coefficient (or mass diffusivity) of the scalar C which is a property of the fluid and introduces the Schmidt number. For laminar flows, the diffusion coefficient D is calculated as the ratio between the kinematic viscosity ν and the Schmidt number ($Sc = \nu/D$). However, as the CO_2 released from the burners is completely turbulent and by similarly to what is done for the turbulent viscosity in turbulent isothermal flows, here an eddy diffusivity D_t and so a turbulent Schmidt number $Sc_t = \nu_t/D_t$ are introduced. In the present case, $D_{eff} = D_t + D$. The turbulent viscosity and the turbulent Schmidt number are evaluated directly from the two-equation turbulence model k-ω SST.

The developed solver has been validated successfully against the numerical results of a heated cavity [14] and CO_2 plume dispersion [15]. More details of the validations could be found in the previous study of Benchikh Le Hocine et $al.$ [16].

Numerical parameters

The developed OpenFoam solver was used to perform the simulations of the different configurations. For the spatial discretization, a fully second-order scheme is selected to reduce numerical dissipation and to model accurately the CO_2 spatial distribution. The Laplacian and the gradient terms are discretized with a bounded Gauss linear numerical scheme. The linear interpolation scheme was used. The pressure-velocity coupling is solved by the SIMPLE (Semi-Implicit-Method for Pressure-Linked Equations) algorithms. The generalised geometric-algebraic multi-grid (GAMG) solver with the combined Diagonal incomplete-Cholesky/Gauss Seidel (symmetric) smoother are considered to solve the pressure and the preconditioned bi-conjugate gradient (PBiCG) solver with Di-

agonal incomplete-LU (DILU) pre-conditioner are employed to solve the rest of the discretized equations.

A two-equation eddy viscosity model named Shear Stress Transport $k-\omega$ ($k-\omega$ SST) developed by Menter [17] is used to model the turbulent flow within the kitchen for the different configurations. The selected turbulence model has the ability to combine the $k-\omega$ Wilcox model formulation [18] in the near-wall region and the $k-\varepsilon$ far from the wall with a blending function. The resulting model shows less sensitivity to free stream conditions, and avoid excessive turbulence kinetic energy levels near stagnation points. The $k-\omega$ SST model has been validated successfully for different configurations and applications [19]–[21].

Concerning the boundary conditions, an air mass flow rate of $0.0566\ kg/s$ and a temperature of 293 K are imposed at each of the three inlets. A uniform turbulence intensity of 5% was also imposed. An inlet mass flow rate condition of $0.0047\ kg/s$ and 100% of CO_2 fraction at a temperature of 400 K are also imposed at the corresponding burner for each configuration. The surrounding walls of the kitchen are considered no slip wall and adiabatic. A simple pressure outlet is imposed at the outlet surface of the pipe.

The inlet and outlet interfaces of the rotor (Fig. 3c) are modeled by an arbitrary mesh interface (AMI), which is modeled using the multiple reference frame (MRF) approach. The MRF approach has already been successfully used for a horizontal axis wind turbine [22].

An unstructured fine grid mesh was generated by using the commercial software Ansys ICEM (Fig. 3). The mesh is composed of tetrahedral elements in the kitchen and rotor regions. The fan blades were reconstructed using 10 prismatic layers. A stretching factor of 1.1 is imposed in the prismatic layers region to respect the maximum aspect ratio for openFoam. For an accurate capture of the CO_2 distribution in the region between the burner and the hood and in the hood and the rotor regions a local refinements are employed. The total number of elements is around 6 millions in the whole kitchen and approximately 1.4 million cell elements in the rotor region (Fig. 3) with a maximum wall coordinate $\max(y^+) < 0.9$ which fulfills the low-Reynolds number approach conditions. A grid sensitivity analysis (not shown here for sake of brevity) has also been performed using two coarser meshes of 1.5 and 3.2 million cells. A discrepancy of 15% and 9% was observed between the 1.5 and 3.2 million cell meshes and the 3.2 and 6 million cell meshes, respectively. The finer mesh is selected to model accurately the CO_2 transport in the kitchen.

RESULTS

Before comparing the hood efficiency in the four configurations, an efficiency study is carried for the hood in configuration 1 for different flow rate. The capture efficiency of the hood is calculated according to the norm E3087−18 [13] as follows:

$$Efficiency = \frac{C_{outlet} - C_{Chamber}}{C_{outlet} - C_{inlet}} \qquad (2)$$

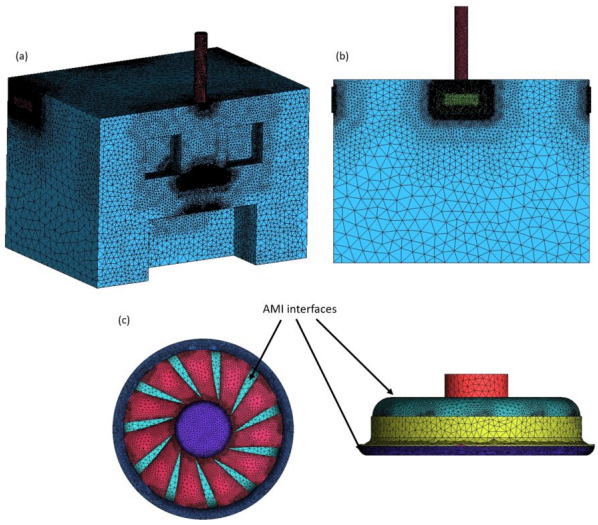

Fig. 3. Different views of mesh distribution: (a) isometric view; (b) front view; (c) rotating domain with the blades.

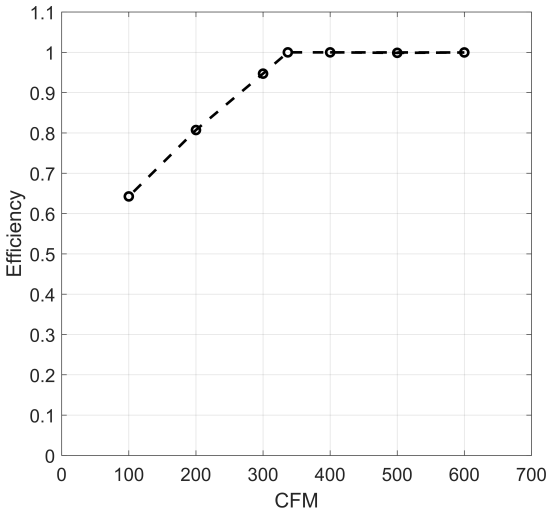

Fig. 4. Variation of the CO_2 capture efficiency.

C_{outlet} and C_{inlet} are the CO_2 concentration at the outlet and inlet, respectively. $C_{chamber}$ is the CO_2 concentration at a specific position inside the kitchen which is determined at the initial time according to the norm E3087−18. In order to test the efficiency of the hood fan, different fan flow rates are considered: 100, 300, 400 and 600 cfm (cubic feet per minute). Each calculation is initialized by the result field obtained for the lower cfm value, respectively.

Figure 4 shows the capture efficiency of the fan in configuration 1 for different suction flow rate. A linear relation is observed between the capture efficiency and the flow rates in the range 100 cfm to 337 cfm. An asymptotic distribution is reached above the flow rate 337 cfm, where a complete capture

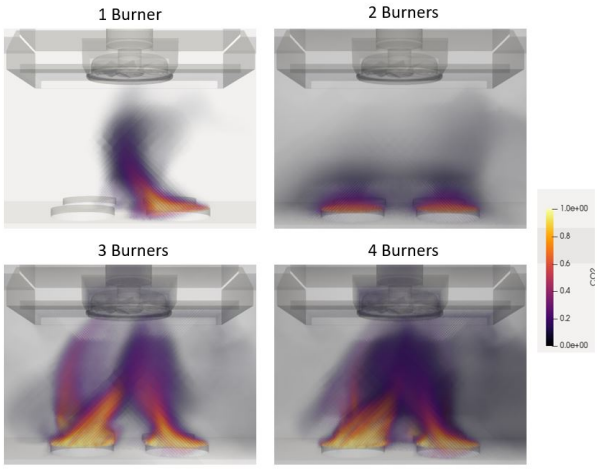

Fig. 5. Front views of the CO_2 distribution for the four configurations.

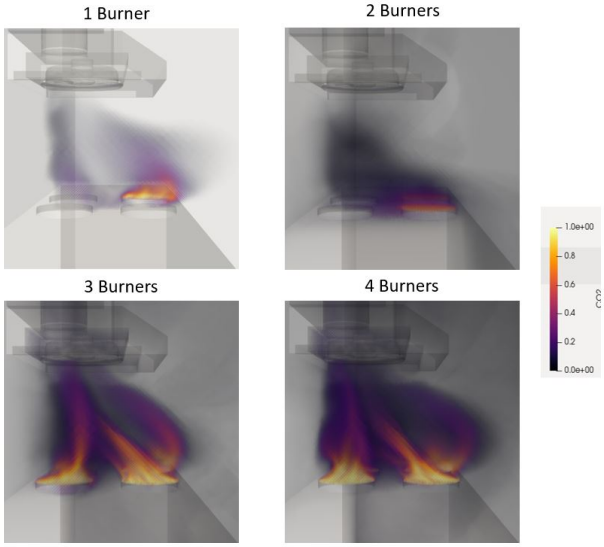

Fig. 6. Lateral views of the CO_2 distribution for the four configurations.

of the released CO_2 is achieved. For flow rates between 400 cfm and 600 cfm, the capture efficiency is totally insensitive as all the released CO_2 is already captured at a lower volume flow rate. As 100% of the capture efficiency is reached at 337 cfm, this flow rate is selected to compare between the four configurations.

In order to understand the capture dynamics of the CO_2 in the four configurations, the front and lateral views of the CO_2 voluminal fraction distribution are presented in fig. 5 and fig. 6, respectively. In configuration 1, the released pollutant follows an arc pattern toward the fan (fig. 5). However, a variation in the CO_2 pattern released from burner 1 is observed when the other burners are turned on (configuration 2, 3 and 4), which is due to the presence of a neighbor jet flow. As all the burners are on in configuration 4, the CO_2 jets tend to collapse near to the hood region in the front view fig. 5 and near to the bottom wall in the lateral view fig. 6. In configuration 2, the CO_2 is scattered non-uniformly in the region between the burners and the hood, however, by turning the burner 3 on in configuration 3 the CO_2 follows the main stream pattern fig. 6. In the lateral views, the pollutant is following a pattern along the bottom wall, where most of the CO_2 is captured through the back section of the fan near to the bottom wall fig. 6.

The capture efficiency of the hood for the four configurations is presented in Table I. A decrease in the capture efficiency is recorded in configuration 2, where a scattered distribution of the CO_2 was observed in fig. 5 . However, in configurations 3 and 4 the capture efficiency is increased to 95 % and 94 %, respectively. The increase of the capture efficiency in configurations 3 and 4, correlates with the pollutant distribution in the lateral views fig. 6 and front views fig. 5, where a main pattern is distinguishable towards the fan.

The temperature distribution at the inlet region of the fan is presented in figure 7 for the four configurations. A discrepancy in the temperature distribution is distinguishable between the different configurations, which correlates with the variation of the CO_2 flow pattern (fig. 6, fig. 5). For configuration 2, the temperature distribution is uniform with a maximum temperature value of 296 K. However, in the other configurations, a non-uniform distribution is observed with higher temperature values near to the bottom walls. By turning on more burners as in configuration 4, the region with higher temperature values is extended due to the increase of the CO_2 flow rate.

TABLE I
CAPTURE EFFICIENCY OF THE TESTED CONFIGURATIONS.

Configurations	Config. 1	Config. 2	Config. 3	Config. 4
Efficiency	100 %	75 %	95 %	94 %

II. CONCLUSION

In the present study a new flow solver based on the $k-\omega$ SST turbulence model and a scalar transport equation for CO_2 was implemented in openFoam to model the CO_2 capture by a hood fan in a realistic residential kitchen. Different burners ignition combinations were tested. The released CO_2 from the burner was characterized by a fixed mass flow rate ($0.0047\ kg/s$) and temperature (400 K).

In configuration 1, a linear relation was observed between the capture efficiency and the flow rate in the range between 100 cfm and 337 cfm. A total capture efficiency of 100% is reached for flow rates above 337 cfm. Above that value, the capture efficiency does not evolve any more.

the CO_2 spatial distribution in the four configurations follows a main pattern toward the fan by passing along the bottom wall. However, in configuration 2 a non-uniform scattered distribution of the pollutant is observed. By turning on the other burners in configurations 3 and 4, the CO_2 follows a more specific pattern. In configuration 4 all the CO_2 jets collapse near the hood entrance. A discrepancy in the

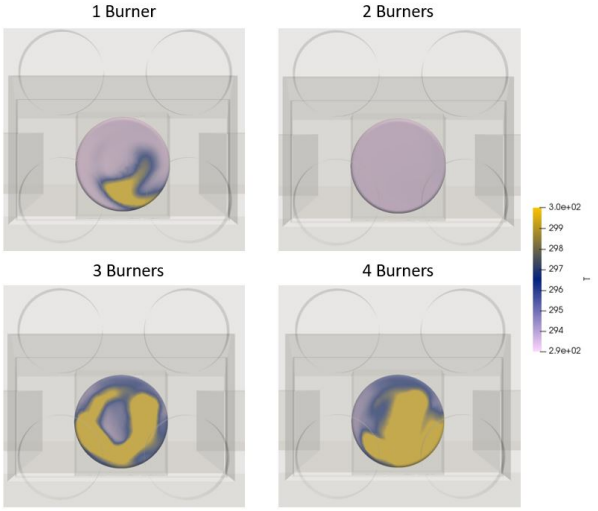

Fig. 7. Bottom views of the temperature distribution for the four configurations at the fan inlet region.

temperature distribution near to the inlet of the rotor region is observed between the different configurations. The region with higher temperature values is extended due to the increase of the CO_2 flow rate.

In a close future, similar modeling will be achieved for different fan configurations. 3D LES simulations are also important to capture accurately the flow dynamics in the hood region. Taking into account the human presence in the numerical simulation is a future perspective to estimate the thermal comfort.

III. ACKNOWLEDGMENT

All calculations have been done using the computational resources of the Compute Canada network, which is here gratefully acknowledged.

REFERENCES

[1] L. Wang, Z. Xiang, S. Stevanovic, Z. Ristovski, F. Salimi, J. Gao, H. Wang, and L. Li, "Role of chinese cooking emissions on ambient air quality and human health," *Science of The Total Environment*, vol. 589, pp. 173 – 181, 2017.

[2] J. Hou, H. Sun, Y. Zhou, Y. Zhang, W. Yin, T. Xu, J. Cheng, W. Chen, and J. Yuan, "Environmental exposure to polycyclic aromatic hydrocarbons, kitchen ventilation, fractional exhaled nitric oxide, and risk of diabetes among chinese females," *Indoor Air*, vol. 28, no. 3, pp. 383–393, 2018.

[3] Y. Zhou, Y. Zou, X. Li, S. Chen, Z. Zhao, F. He, W. Zou, Q. Luo, W. Li, Y. Pan, X. Deng, X. Wang, R. Qiu, S. Liu, J. Zheng, N. Zhong, and P. Ran, "Lung function and incidence of chronic obstructive pulmonary disease after improved cooking fuels and kitchen ventilation: A 9-year prospective cohort study," *PLOS Medicine*, vol. 11, no. 3, pp. 1–11, 03 2014.

[4] K. Yu, K. Yang, Y. Chen, J. Y. Gong, Y. P. Chen, H. Shih, and S. C. Lung, "Indoor air pollution from gas cooking in five taiwanese families," *Building and Environment*, vol. 93, pp. 258 – 266, 2015.

[5] C. Cao, J. Gao, L. Wu, X. Ding, and X. Zhang, "Ventilation improvement for reducing individual exposure to cooking-generated particles in Chinese residential kitchen," *Indoor and Built Environment*, vol. 26, 10 2016.

[6] K. Yi, Y. Kim, and G. N. Bae, "Effect of air flow rates on concurrent supply and exhaust kitchen ventilation system," *Indoor and Built Environment*, vol. 25, 01 2014.

[7] L. Tseng and C. Chen, "Effect of Flow Characteristics on Ultrafine Particle Emissions from Range Hoods," *The Annals of Occupational Hygiene*, vol. 57, no. 7, pp. 920–933, 03 2013.

[8] S. M. Lee and J. W. Lee, "Performance of the vortex ventilator system based on capture velocity and capture efficiency," *HVAC&R Research*, vol. 12, no. sup3, pp. 889–901, 2006.

[9] R. F. Huang, G. Z. Dai, and J. K. Chen, "Effects of Mannequin and Walk-by Motion on Flow and Spillage Characteristics of Wall-Mounted and Jet-Isolated Range Hoods," *The Annals of Occupational Hygiene*, vol. 54, no. 6, pp. 625–639, 04 2010.

[10] Y. Cao, Y. Wang, C. Li, J. Ding, Y. Yang, and X. Ren, "A field measurement study of a parallel-flow pushpull system for industrial ventilation applications," *International Journal of Ventilation*, vol. 15, no. 2, pp. 167–181, 2016.

[11] Y. Wang, Y. Huang, Y. Zhou, Y. Shu, and J. Liu, "Experimental study on one-side confined jets from a parallel-flow outlet in a push-pull ventilation system," *Indoor and Built Environment*, vol. 24, pp. 73–86, 01 2013.

[12] B. Zhou, F. Chen, Z. Dong, and P. V. Nielsen, "Study on pollution control in residential kitchen based on the push-pull ventilation system," *Building and Environment*, vol. 107, pp. 99 – 112, 2016.

[13] "Standard Test Method for Measuring Capture Efficiency of Domestic Range Hoods." ASTM International, Standard, 2018.

[14] P. V. Nielsen, "Prediction of air flow and comfort in air conditioned spaces," *ASHRAE Transactions*, vol. 81, pp. 247–259, 1975, vol. 81, Part II.

[15] J. Xing, Z. Liu, P. Huang, C. Feng, Y. Zhou, D. Zhang, and F. Wang, "Experimental and numerical study of the dispersion of carbon dioxide plume," *Journal of Hazardous Materials*, vol. 256-257, pp. 40 – 48, 2013.

[16] A. E. Benchikh Le Hocine, S. Poncet, and H. Fellouah, "Numerical investigation of the capture efficiency of a domestic range hood," ser. ASME Summer heat transfer conference, vol. Submitted, Rosen Shingle Creek, Orlando, FL USA, 07 2020.

[17] F. R. Menter, "Two-equation eddy-viscosity turbulence models for engineering applications," *AIAA Journal*, vol. 32, no. 8, pp. 1598–1605, 1994.

[18] D. C. Wilcox, "Reassessment of the scale-determining equation for advanced turbulence models," *AIAA Journal*, vol. 26, no. 11, pp. 1299–1310, 1988.

[19] J. E. Bardina, P. G. Huang, and T. J. Coakley, "Turbulence Modeling, Validation, Testing and Development," NASA Technical Memorandum 110446, Tech. Rep., 1997.

[20] A. E. Benchikh Le Hocine, R. W. J. Lacey, and S. Poncet, "Multiphase modeling of the free surface flow through a Darrieus horizontal axis shallow-water turbine," *Renewable Energy*, vol. 143, pp. 1890 – 1901, 2019.

[21] A. E. Benchikh Lehocine, R. W. J. Lacey, and S. Poncet, "Turbulent flow over a D-section bluff body: a numerical benchmark," *Environmental Fluid Mechanics*, vol. 19, no. 2, pp. 435–456, 2019.

[22] Y. Zhang, S. Deng, and X. Wang, "Rans and ddes simulations of a horizontal-axis wind turbine under stalled flow condition using openfoam," *Energy*, vol. 167, pp. 1155 – 1163, 2019.